

# Digital image correlation data from laboratory subduction megathrust models

(<https://doi.org/10.5880/fidgeo.2022.015>)

---

Ehsan Kosari <sup>1,2</sup>, Matthias Rosenau <sup>1</sup>, Onno Oncken <sup>1,2</sup>

1. GFZ German Research Centre for Geosciences, Potsdam, Germany
2. Department of Earth Sciences, Freie Universität Berlin, Berlin, Germany.

## 1. Licence

Creative Commons Attribution 4.0 International License (CC BY 4.0)



## 2. Citation

**When using the data, please cite it like:**

Kosari, Ehsan; Rosenau, Matthias; Oncken, Onno (2022): Digital image correlation data from laboratory subduction megathrust models. GFZ Data Services. <https://doi.org/10.5880/fidgeo.2022.015>

**The data are supplementary material to:**

Kosari, E., Rosenau, M., & Oncken, O. (2022). Strain signals governed by frictional-elastoplastic interaction of the upper plate and shallow subduction megathrust interface over seismic cycles. In Tectonics. American Geophysical Union (AGU). <https://doi.org/10.1029/2021tc007099>

## Table of contents

1. Licence.....	1
2. Citation .....	1
Table of contents.....	1
3. Data Description.....	2
3.1. Experimental setup .....	2
3.2. Digital image correlation .....	3
4. File description .....	4
4. References.....	5

### 3. Data Description

This data set includes digital image correlation data from analog earthquakes experiments. The data consists of grids of surface strain and time series of surface displacement (horizontal and vertical) and strain. The data have been derived using a stereo camera setup and processed with LaVision Davis 10 software. Detailed descriptions of the experiments and results regarding the surface pattern of the strain can be found in Kosari et al. (2022), to which this data set is supplementary.

#### 3.1. Experimental setup

We use an analog seismotectonic scale model approach (Rosenau et al., 2019 and 2017) to generate a catalog of analog megathrust earthquakes (Table 1). The presented experimental setup is modified from the 3D setup used in Rosenau et al. (2019) and Kosari et al. (2020). The subduction forearc model wedge is set up in a glass-sided box (1000 mm across strike, 800mm along strike, and 300 mm deep) with a dipping, elastic basal conveyor belt and a rigid backwall. An elastoplastic sand-rubber mixture (50 vol.% quartz sandG12: 50 vol.% EPDM rubber) is sieved into the setup representing a 240 km long forearc segment from the trench to the volcanic arc. The shallow part of the wedge includes a basal layer of sticky rice grains characterized by unstable stick-slip sliding representing the seismogenic zone. Stick-slip sliding in rice is governed by a rate-and-state dependent friction law similar to natural rocks.

According to Coulomb wedge theory, two types of wedge configurations have been designed: a “compressional” configuration represents an interseismically compressional and coseismically stable wedge (compressional configuration), and a “critical” configuration, which is interseismically stable (close to critically compressional) and may reach a critical extensional state coseismically (critical configuration). In the compressional configuration, a flat-top (surface slope  $\alpha=0$ ) wedge overlies a single large rectangular in map view stick-slip patch (Width\*Length=200\*800 mm) over a 15-degree dipping basal thrust. In the critical configuration, the surface angle of the elastoplastic wedge varies from the coastal segment onshore ( $\alpha=10$ ) to the inner-wedge offshore ( $\alpha=15$ ) segments over a 5-degree dipping basal thrust. Slow continuous compression of the wedge by moving the basal conveyor belt at a speed velocity of 0.05 mm/s simulates plate convergence and results in the quasi-periodic nucleation of quasi-periodic stick-slip events (analog earthquakes) within the rice layer. The wedge responds elastically to these basal slip events, similar to crustal rebound during natural subduction megathrust earthquakes.

**Table 1: Examples of surface displacement time-series from two different configurations. The values are at a laboratory scale.**

t(sec)	compressional Configuration	Critical Configuration
	Vx(mm)	Vx(mm)
1500	-0,03	-0,02
1501	-0,02	-0,02
1502	-0,02	-0,02
1503	-0,03	0,19
1504	-0,02	-0,03
1505	-0,02	-0,02
1506	-0,02	-0,02
1507	0,16	-0,02
1508	-0,01	-0,02
1509	-0,03	-0,02
1510	-0,02	-0,02

### 3.2. Digital image correlation

To monitor the surface deformation of the wedge analog model, a stereoscopic set of two CCD cameras (LaVision Imager pro X 11MPx, 14 bit) monitors images of the wedge surface continuously at 4 Hz. To derive observational data similar to those from geodetic techniques, i.e., velocities at the location on the surface, we use digital image correlation (DIC; Adam et al., 2005) to derive the 3D incremental surface displacement (or velocity) at high spatial resolution. To calculate strain (Figure 1), we use the infinitesimal strain tensor because the condition of small strain is met when resolving strains across the forearc during the interseismic period:

$$\begin{pmatrix} \varepsilon_{xx} & \varepsilon_{xy} & \varepsilon_{xz} \\ \varepsilon_{yx} & \varepsilon_{yy} & \varepsilon_{yz} \\ \varepsilon_{zx} & \varepsilon_{zy} & \varepsilon_{zz} \end{pmatrix}$$

where  $\varepsilon_{xx}$  represent the partial derivation of the trench-normal surface velocity component  $\frac{\partial v_x}{\partial x}$  showing trench-normal shortening: positive and negative values respectively represent compression and extension.

The time series of incremental surface displacement data (Figure 2 and Table 2) and the strain (Figure 2) are calculated using LaVision Davis 10 software. The result is an evenly spaced grid of vectors per time step, oriented parallel with respect to the principal dimensions of the box.

We applied the Least Squares method-based 3D algorithm using smaller image subsets (subset size: 95 px) with overlap (step size: 31 px) to gain dense 3D deformation fields followed by post-processing, including the filtering and smoothing steps.

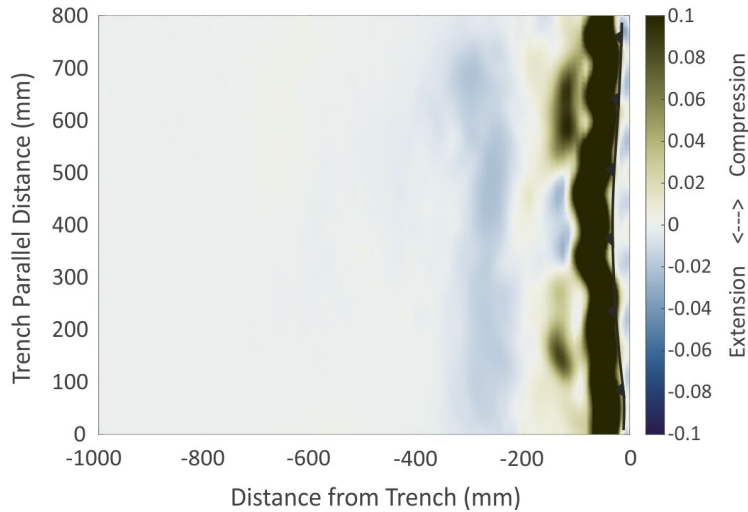


**Figure 1: Example of surface strain pattern from the critical configuration.**

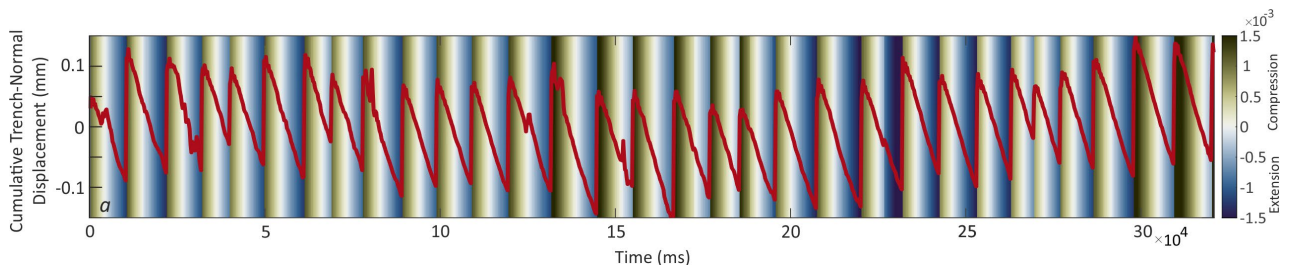


**Figure 2: Example of strain (background colormap) and tranch-normal displacement (red line plot) time series from the critical configuration.**

## 4. File description

The folder “2022-015\_Kosari-et-al\_Data.zip” includes 20 files in .csv format:

- **2022-015\_Kosari-et-al\_Data\_compressional-config:** Time-series from compressional configuration over tens of seismic cycles
- **2022-015\_Kosari-et-al\_Data\_critica-config:** Time-series from critical configuration over tens of seismic cycles
- **2022-015\_Kosari-et-al\_Data\_High-res- compressional-(Vz):** High resolution (3 cycles) vertical displacement from compressional config. as a grid file.
- **2022-015\_Kosari-et-al\_Data\_High-res-compressional:** High resolution (3 cycles) strain from compressional config. as a grid file.
- **2022-015\_Kosari-et-al\_Data\_High-res-critical-(Vz):** High resolution (3 cycles) vertical displacement from critical config. as a grid file.
- **2022-015\_Kosari-et-al\_Data\_High-res-critical:** High resolution (3 cycles) strain from critical config. as a grid file.
- **2022-015\_Kosari-et-al\_Data\_Intermediate-res-compressional-(Vz):** Intermediate resolution (3 cycles) vertical displacement from compressional config. as a grid file.
- **2022-015\_Kosari-et-al\_Data\_Intermediate-res-compressional:** Intermediate resolution (9 cycles) strain from compressional config. as a grid file.
- **2022-015\_Kosari-et-al\_Data\_Intermediate-res-critical-(Vz):** Intermediate resolution (3 cycles) vertical displacement from critical config. as a grid file.
- **2022-015\_Kosari-et-al\_Data\_Intermediate-res-critical:** Intermediate resolution (9 cycles) strain from critical config. as a grid file.
- **2022-015\_Kosari-et-al\_Data\_Low-res-compressional-(Vz):** Low resolution (3 cycles) vertical displacement from compressional config. as a grid file.
- **2022-015\_Kosari-et-al\_Data\_Low-res-compressional:** Low resolution (18 cycles) strain from compressional config. as a grid file.
- **2022-015\_Kosari-et-al\_Data\_Low-res-critical-(Vz):** Low resolution (3 cycles) vertical displacement from critical config. as a grid file.
- **2022-015\_Kosari-et-al\_Data\_Low-res-critical:** Low resolution (18 cycles) strain from critical config. as a grid file.
- **2022-015\_Kosari-et-al\_Data\_Map-view-compressional-config-s:** Map view of the strain pattern from compressional config. as a grid file.
- **2022-015\_Kosari-et-al\_Data\_Map-view\_compressional-config-Vz:** Map view of the vertical displacement from compressional config. as a grid file.
- **2022-015\_Kosari-et-al\_Data\_Map-view-critical-config-s:** Map view of the strain pattern from critical config. as a grid file.
- **2022-015\_Kosari-et-al\_Data\_Map-view-critical-config-Vz:** Map view of the vertical displacement from the critical config. as a grid file.
- **2022-015\_Kosari-et-al\_Data\_time-series-compressional-config:** Trench-normal displacement time series from the critical configuration.
- **2022-015\_Kosari-et-al\_Data\_time-series-critical-config:** Trench-normal displacement time series from the critical configuration.

**Table 2: Example of time-series data file (9 columns out of 1286 from critical configuration).**

	Outer-wedge		Inner-wedge		coast		Outer-wedge	Inner-wedge	coast
time	Vz	Vx	Vz	Vx	Vz	Vx	time	Vz	Vx
0	-0,02	-0,08	-0,02	-0,07	0,01	-0,06	0	-0,02	-0,08
250	0,02	0,05	0,02	0,06	-0,02	0,03	250	0,02	0,05
500	0,02	0,04	0,02	0,04	-0,02	0,01	500	0,02	0,04
750	0,02	0,04	0,02	0,04	-0,02	0,01	750	0,02	0,04
1000	0,01	0,05	0,01	0,04	-0,03	0,01	1000	0,01	0,05
1250	0,01	0,04	0,01	0,03	-0,03	0,00	1250	0,01	0,04
1500	0,01	0,04	0,01	0,03	-0,02	0,01	1500	0,01	0,04
1750	0,01	0,03	0,01	0,02	-0,02	0,00	1750	0,01	0,03
2000	0,01	0,03	0,01	0,02	-0,02	0,00	2000	0,01	0,03

## 4. References

- Adam, J., Urai, J. L., Wienke, B., Oncken, O., Pfeiffer, K., Kukowski, N., Lohrmann, J., Hoth, S., van der Zee, W & Schmatz, J. (2005). Shear localisation and strain distribution during tectonic faulting – New insights from granular-flow experiments and high-resolution optical image correlation techniques. *Journal of Structural Geology*, 27(2), 283–301, <https://doi.org/10.1016/j.jsg.2004.08.008>
- Kosari, E., Rosenau, M., Bedford, J., Rudolf, M., & Oncken, O. (2020). On the relationship between offshore geodetic coverage and slip model uncertainty: Analog megathrust earthquake case studies. *Geophysical Research Letters*, 47(15), <https://doi.org/10.1029/2020GL088266>
- Kosari, E., Rosenau, M., & Oncken, O. (2022). Strain signals governed by frictional-elastoplastic interaction of the upper plate and shallow subduction megathrust interface over seismic cycles. In *Tectonics*, <https://doi.org/10.1029/2021tc007099>
- Rosenau, M., Corbi, F., & Dominguez, S. (2017). Analogue earthquakes and seismic cycles: experimental modelling across timescales. *Solid Earth*, European Geosciences Union. 8(3), 597–635. <https://doi.org/10.5194/se-8-597-2017>
- Rosenau, M., Horenko, I., Corbi, F., Rudolf, M., Kornhuber, R., & Oncken, O. (2019). Synchronization of Great Subduction Megathrust Earthquakes: Insights From Scale Model Analysis. *Journal of Geophysical Research: Solid Earth*, 124(4), 3646–3661. <https://doi.org/10.1029/2018JB016597>